

4.4 Design Publications

Introduction

Please find attached to this section, two papers on reinforced concrete masonry walls:

1. *Experimental In-Plane Shear Strength Investigation of Reinforced Concrete Masonry Walls*, written by K. C. Voon and J. M. Ingham, published in the March 2006 Journal of Structural Engineering.
2. *Experimental In-Plane Strength Investigation of Reinforced Concrete Masonry Walls with Openings*, written by K. C. Voon and J. M. Ingham, published in the May 2008 Journal of Structural Engineering.

Copyright and Disclaimer

© 2010 New Zealand Concrete Masonry Association Inc.

Except where the Copyright Act and the Limited-License Agreement allows otherwise, no part of this publication may be reproduced, stored in a retrieval system in any form or transmitted by any means without prior permission in writing of the New Zealand Concrete Masonry Association. The information provided in this publication is intended for general guidance only and in no way replaces the services of professional consultants on particular projects. No liability can therefore be accepted, by the New Zealand Concrete Masonry Association, for its use. For full terms and conditions see <http://www.nzcma.org.nz/manual.html>.



Experimental In-Plane Shear Strength Investigation of Reinforced Concrete Masonry Walls

K. C. Voon¹ and J. M. Ingham²

Abstract: This paper presents test results of ten single-story reinforced concrete masonry shear walls. Test results are summarized and compared with design formulae specified by the New Zealand masonry design standard NZS 4230:1990 and by the National Earthquake Hazards Reduction Program. It was determined that the test walls exhibited shear strength significantly exceeding the NZS 4230:1990 maximum permissible shear stress, confirming that NZS 4230:1990 was overly conservative in accounting for masonry shear strength. It was also confirmed from the test results that masonry shear strength increases with the magnitude of applied axial compressive stress and the amount of shear reinforcement, but that the shear strength decreases inversely in relation to an increase in wall aspect ratio. In addition, it was shown that the postcracking performance of shear dominated walls was substantially improved when uniformly distributing the shear reinforcement up the height of the walls.

DOI: 10.1061/(ASCE)0733-9445(2006)132:3(400)

CE Database subject headings: Concrete masonry; Walls; Shear strength; Grouting; Reinforcement; Axial loads.

Introduction

Masonry has been used as a common construction material worldwide for many centuries. However, the vulnerability of unreinforced masonry systems was highlighted during past and recent earthquakes. Consequently, reinforcement was introduced to masonry shear walls to resist lateral forces generated in regions of high seismic activity. These walls are usually subjected to simultaneous gravity and lateral loads, resulting in overturning moments during seismic excitation. Depending on the load condition, the amount of longitudinal and shear reinforcement, and the aspect ratio, two types of failure mechanisms can be identified in masonry shear wall panels subjected to in-plane loading. One is a flexural type of failure, which is characterized by the tensile yielding of vertical reinforcement or crushing of masonry at critical wall sections. This is generally the preferred mode, as tensile failure is ductile and is effective in dissipating energy in conjunction with reinforcement yielding. The second type is a shear failure, which is characterized by diagonal tensile cracking. Wall panels that fail predominantly in a shear mode exhibit brittle behavior, characterized by rapid strength degradation soon after the maximum strength is developed. In order to prevent such catastrophic failure, New Zealand was amongst the first countries to develop reinforced masonry seismic design procedures based on

the principle of capacity design (Priestley 1980) that required the dependable shear strength to exceed the maximum lateral loading necessary to develop the wall flexural overstrength.

At the time the New Zealand masonry design standard NZS 4230:1990 was released, it was recorded in the associated commentary that the shear strength provisions in this standard were overly conservative. However, the absence at that time of experimental data related to the shear strength of masonry walls when subjected to in-plane seismic forces prevented the preparation of more accurate criteria. A comprehensive literature review conducted by the authors indicated that since the release of NZS 4230:1990, many experimental studies have been carried out worldwide to investigate the in-plane shear capacity of reinforced masonry shear walls. It was demonstrated that the shear resistance of reinforced masonry walls comes from several mechanisms, such as tension of horizontal reinforcement, dowel action of vertical reinforcement, applied axial stress, and aggregate interlocking. Although some researchers observed that the shear strength of a wall panel is not directly proportional to the amount of horizontal reinforcement present (Mayes et al. 1976; Chen et al. 1978; Hidalgo et al. 1979; Hiraishi 1985; Sveinsson et al. 1985), the ductility of shear-dominated wall panels was improved by increasing the amount of horizontal reinforcement (Matsumura 1988; Shing et al. 1990). Furthermore, it was demonstrated that horizontal reinforcement can effectively inhibit the opening of diagonal cracks (Priestley 1977).

The New Zealand masonry design standard was recently revised, providing an opportunity to update the masonry shear strength criteria. Therefore, ten single-story concrete masonry wall panels were tested at the University of Auckland in order to examine the in-plane shear strength of concrete masonry walls constructed using New Zealand masonry units utilizing pumice aggregate and assembled using common local construction techniques. The main variables considered in this experimental program included the amount and distribution of shear reinforcement, level of axial compression stress, type of grouting, and wall aspect ratios. This experimental program supplemented the experimental data already available by specifically investigating the

¹PhD Candidate, Dept. of Civil and Environmental Engineering, Univ. of Auckland, Private Bag 92019, Auckland, New Zealand. E-mail: kvoo002@ec.auckland.ac.nz

²Senior Lecturer, Dept. of Civil and Environmental Engineering, Univ. of Auckland, Private Bag 92019, Auckland, New Zealand. E-mail: j.ingham@auckland.ac.nz

Note. Associate Editor: Rob Y. H. Chai. Discussion open until August 1, 2006. Separate discussions must be submitted for individual papers. To extend the closing date by one month, a written request must be filed with the ASCE Managing Editor. The manuscript for this paper was submitted for review and possible publication on August 16, 2004; approved on July 26, 2005. This paper is part of the *Journal of Structural Engineering*, Vol. 132, No. 3, March 1, 2006. ©ASCE, ISSN 0733-9445/2006/3-400-408/\$25.00.

Table 1. Masonry Shear Wall Specimens

Wall	H (mm)	L (mm)	Effective width (mm)	H_e (mm)	H_e/L	Reinforcement		ρ_h (%)	Grouting	Axial stress (MPa)
						Vertical	Horizontal			
1	1,800	1,800	140	1,800	1.0	5-D20	5 \times R6	0.05	Full	—
2	1,800	1,800	140	1,800	1.0	5-D20	1-R6	0.01	Full	—
3	1,800	1,800	140	1,800	1.0	5-D20	5-D10	0.14	Full	—
4	1,800	1,800	140	1,800	1.0	5-D20	2-D10	0.06	Full	—
5	1,800	1,800	60	1,800	1.0	5-D20	—	—	Partial	—
6	1,800	1,800	60	1,800	1.0	3-D20	—	—	Partial	—
7	1,800	1,800	140	1,800	1.0	5-D20	5-R6	0.05	Full	0.50
8	1,800	1,800	140	1,800	1.0	5-D20	5-R6	0.05	Full	0.25
9	3,600	1,800	140	3,600	2.0	5-DH25	9-R6	0.05	Full	0.25
10	1,800	3,000	140	1,800	0.6	8-D20	5-R6	0.05	Full	0.25

shear strength of walls subjected to low axial compression stresses ($\sigma_n \leq 0.50$ MPa) and low shear reinforcement ratios ($\rho_h \leq 0.062\%$). Experimental studies conducted in both the United States and Japan involved masonry walls that were subjected to σ_n and ρ_h of up to 5.9 MPa and 0.67%, respectively.

Experimental Program

Test Specimens

A total of ten concrete masonry cantilever walls were tested. The dimensions and reinforcement details for the ten walls are summarized in Table 1. All walls (except Walls 5 and 6) were fully grouted and had vertical reinforcing steel spaced at 400 mm c/c, but varied in the quantity and positioning of horizontal shear reinforcement. The horizontal shear reinforcing steel was uniformly distributed evenly up the height of the walls and was hooked (180° bend) around the outermost wall vertical reinforcing bars. Walls 5 and 6 were partially grout filled with no horizontal shear reinforcement, and their vertical reinforcement was spaced at 400 mm and 800 mm, respectively. For the two partially grout-filled walls, only cells containing reinforcing bars were filled with grout. Walls 1 to 6 were tested without externally applied vertical axial compression load. Walls 7 and 8 were duplicates of Wall 1,

but with externally applied axial compression stress of 0.5 MPa and 0.25 MPa, respectively. Walls 9 and 10, which were constructed to H_e/L ratios of 2.0 and 0.6, were both subjected to axial compression stress of 0.25 MPa. All test walls (except Wall 3) were designed to have a dominant shear type of failure. Wall 3 was designed to fail in flexure.

All walls were constructed by experienced masons under supervision, and employed a running bond pattern of standard production 15 series (140 mm wide) precast concrete masonry units (CMUs). This width was adopted for the tests to ensure that high shear stresses could be applied within the maximum load restrictions of the hydraulic actuators available at the University of Auckland. Open-end bond beam CMUs having a depressed web were used throughout the wall height to allow the horizontal shear reinforcement to be positioned at all levels and to enhance the continuity of grout. Dricon Trade Mortar—a bagged 1:4 portion of Portland cement and sand by volume—was used throughout. High slump ready-mix grout using small aggregate (7 mm) was employed for filling the cavities within the test walls and a common commercially used expansive chemical additive was added to the grout to avoid formation of voids caused by high shrinkage of the grout. Additional detailed descriptions of the wall panels are reported in Voon and Ingham (2003).

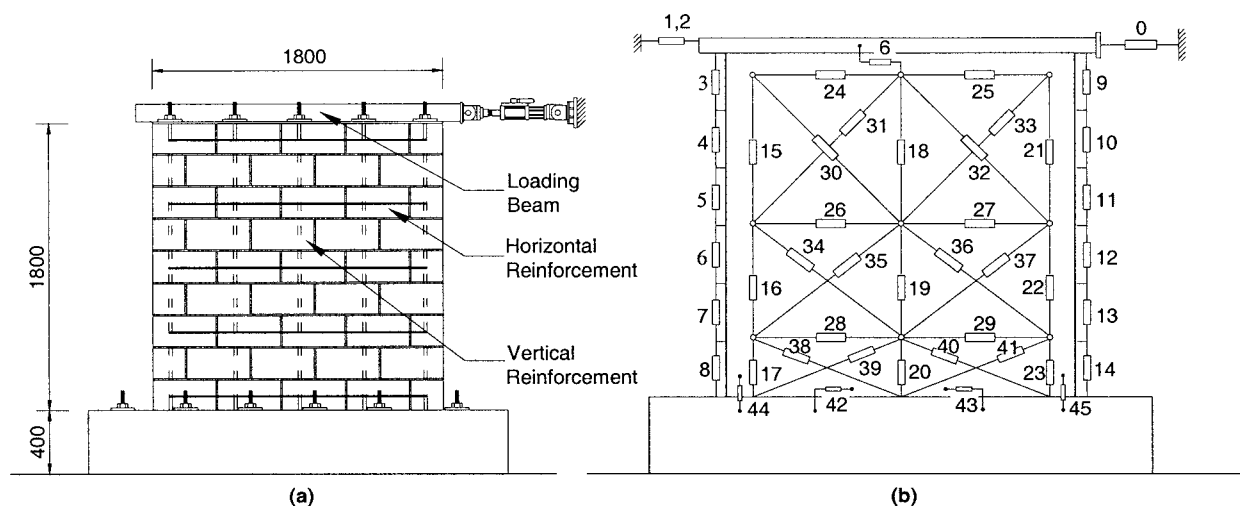
**Fig. 1.** Test setup and instrumentation

Table 2. Summary of Test Results

Wall	f'_m (MPa)	Prediction			Test result				Failure mode
		F_n (kN)	V_n (kN)	$\frac{V_n}{F_n}$	V_{max} (kN)	d_{vmax} (mm)	$\frac{V_{max}}{V_n}$	d_u (mm)	
1	17.6	229	219	0.95	215	10	0.98	12	Flexure/ Shear
2	17.6	229	195	0.85	195	6	1.00	8	Shear
3	17.0	229	250	1.09	215	8	0.86	10	Flexure/ Sliding
4	17.0	229	219	0.95	223	8	1.02	10	Shear
5	18.5	229	91	0.40	143	8	1.57	10	Shear
6	18.5	142	91	0.64	93	8	1.02	14	Shear
7	18.8	282	256	0.91	263	6	1.03	8	Shear
8	18.8	256	240	0.93	244	6	1.02	6	Shear
9	24.3	272	268	0.99	207	20	0.77	24	Shear
10	24.3	672	568	0.85	598	4	1.05	4	Shear

Test Setup and Instrumentation

The test setup is shown in Fig. 1(a), primarily consisting of a reinforced concrete footing and a horizontally mounted hydraulic actuator providing a horizontal shear force to the top of the wall through a 150×75 steel channel section (herein called the loading beam). The wall was stabilized from moving in its out-of-plane direction by two parallel horizontal struts that were positioned perpendicular to the wall and hinged to the channel and a reaction frame. Fig. 1(b) schematically shows typical wall instrumentation. Lateral load was measured by a load cell positioned in series with the hydraulic actuator, denoted as instrument 0 in Fig. 1(b). The lateral displacement at the top of the wall was measured by instruments 1 and 2 (portal type LVDT). Wall flexural and shear deformations were monitored by instruments 3–14 and 15–41, respectively. The base uplift was monitored by instruments 44 and 45, installed very close to the base joint while, relative sliding displacement between the wall and footing was measured by instruments 42 and 43.

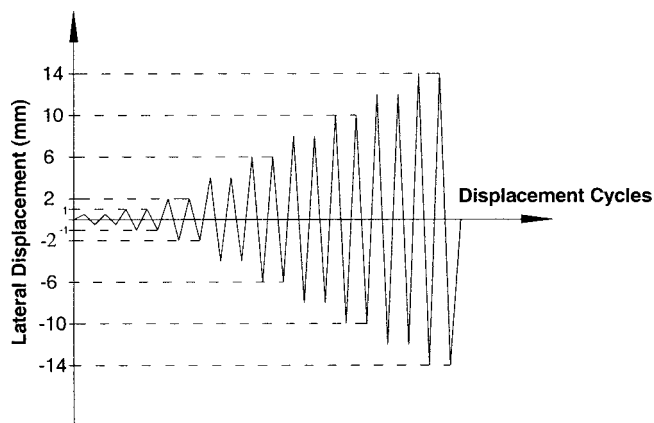
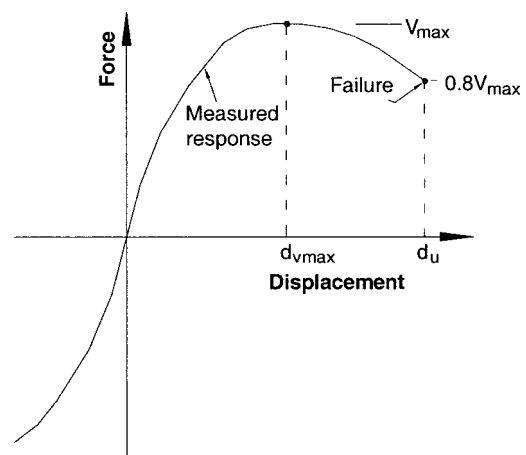
Material Properties

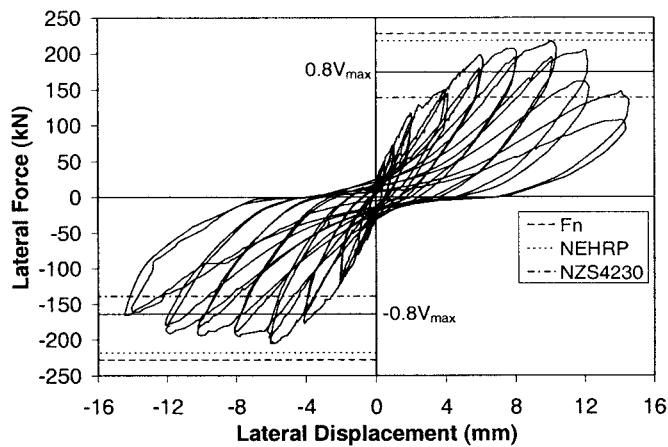
Samples were taken from steel reinforcement used in wall construction. These samples were subjected to tensile testing, with

the average yield strengths (f_y) for the R6, D10, and D20 reinforcing steel being 325, 320, and 318 MPa, respectively. Also, masonry compression strength, f'_m , was determined by material testing of masonry prisms. These prisms were built of three concrete masonry units stacked on top of each other, using the same construction technique as was used for the wall. The prisms were grout filled at the same time as the wall and were then subjected to the same curing condition as the wall panels. The prisms were tested using an Avery universal testing machine. This type of test specimen provided the most accurate estimate of f'_m , with values summarized in Table 2.

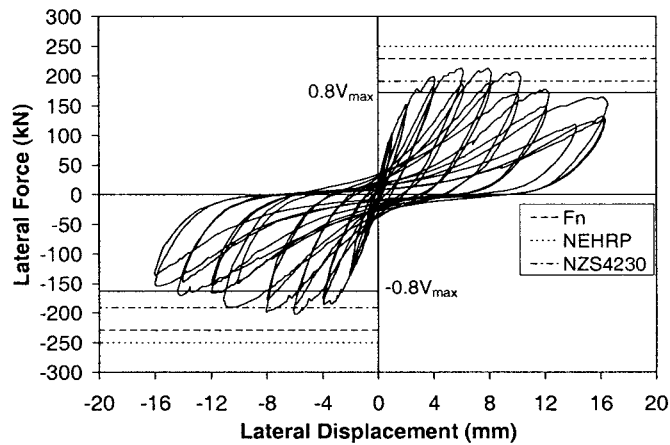
Testing Procedure

The cyclic loading sequence adopted for all tests is shown in Fig. 2, and consisted of a series of displacement-controlled components. Each stage of loading consisted of two cycles to the selected displacement. This experimental program defined failure as the point on the loading curve where the wall strength had reduced to 80% of the maximum strength previously recorded, with d_u as the corresponding ultimate displacement (see Fig. 3).

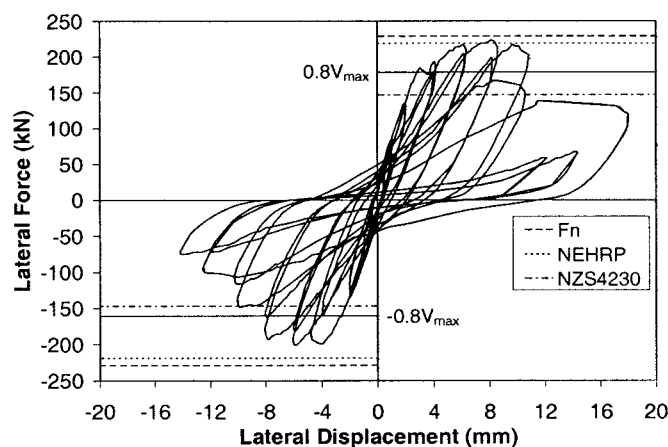
**Fig. 2.** Imposed displacement history**Fig. 3.** Theoretical point of failure



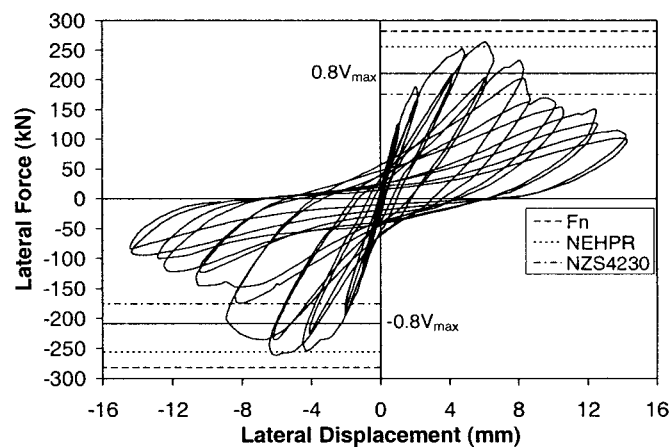
(a) Wall 1



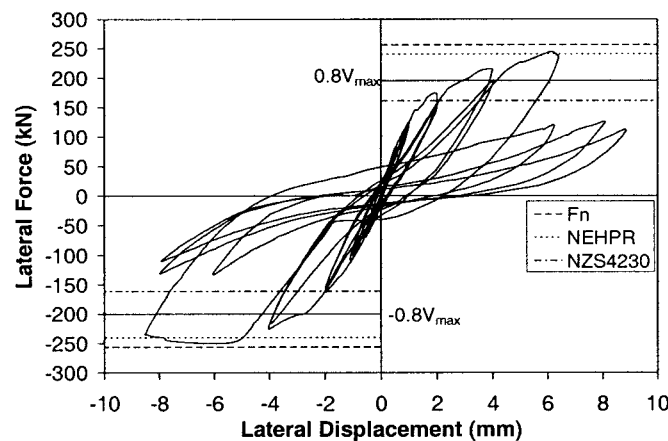
(b) Wall 3



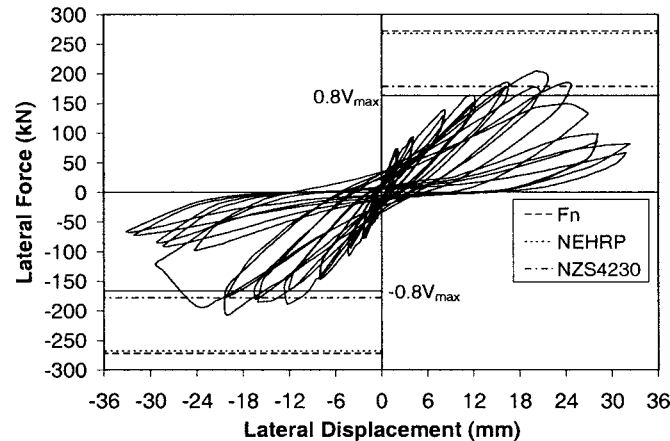
(c) Wall 4



(d) Wall 7



(e) Wall 8



(f) Wall 9

Fig. 4. Force-displacement histories

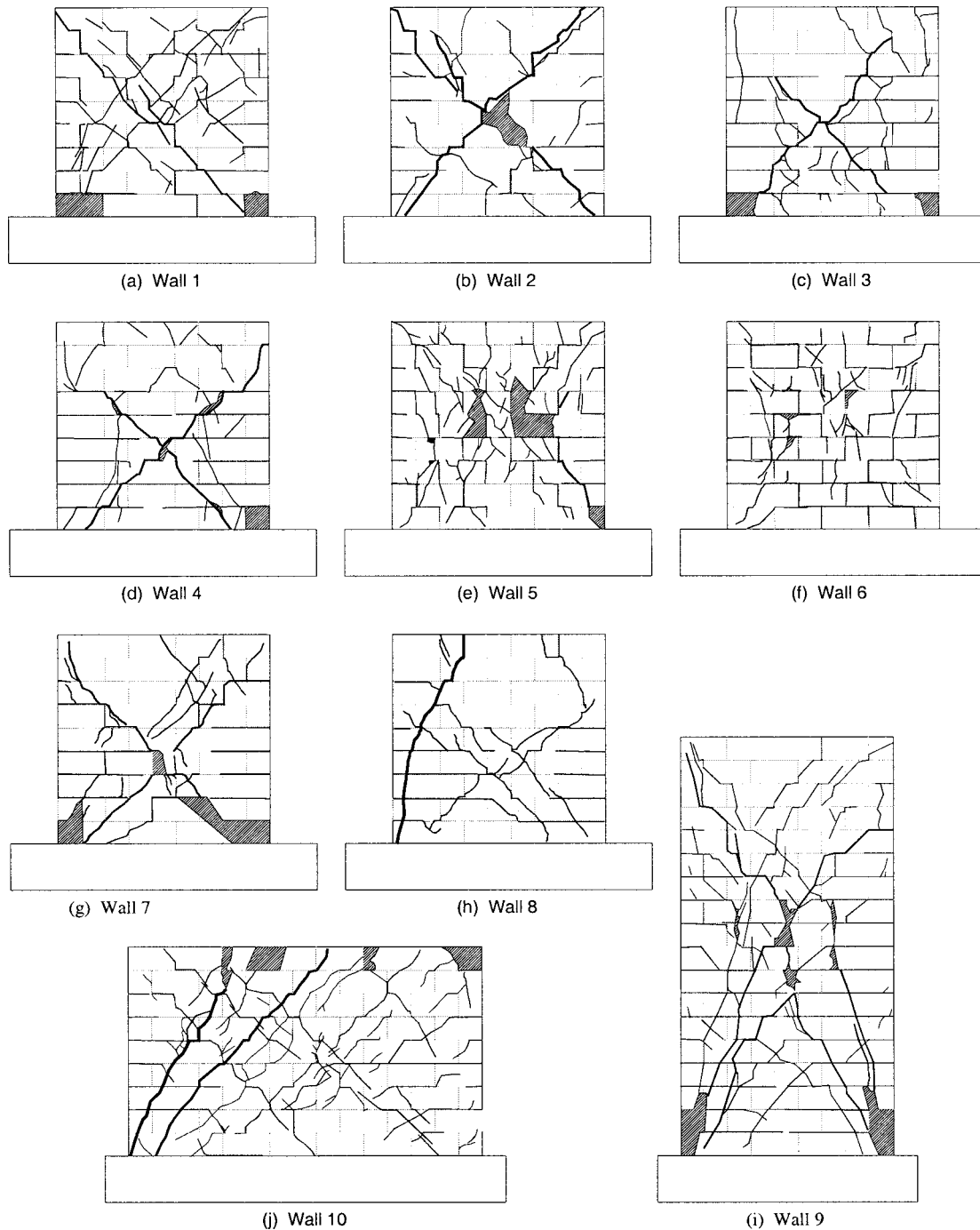


Fig. 5. Masonry wall cracking patterns

The predicted masonry shear strength, V_n , was calculated according to the formulae presented in NZS 4230:1990

$$V_n = 0.8v_m A_n + 0.8\rho_h A_n f_{yh} \quad (1)$$

where v_m is the greater of $v_m = 0.30$ MPa or $v_m = 0.03f'_m + 0.3\sigma_n \leq 0.72$ MPa, with $f'_m \leq 16$ MPa; and also according to NEHRP (1997)

$$V_n = 0.083 \left(4 - 1.75 \frac{H_e}{L} \right) A_n \sqrt{f'_m} + 0.5\rho_h A_n f_{yh} + 0.25\sigma_n A_n \quad (2)$$

Experimental Results

General wall behavior is summarized in Table 2, where V_{max} = maximum lateral force recorded and d_{vmax} = corresponding displacement (see Fig. 3). The predicted masonry shear strength, V_n , listed in Table 2, was based on Eq. (2), being most recently developed and having the ability to predict masonry shear strength with accuracy superior to that of Eq. (1) (Voon and Ingham 2001). The shear strengths of the two partially grouted walls listed in Table 2 were calculated using a common New Zealand approach where the effective section width for shear was assumed to be the net thickness of the face shells only. This limitation was

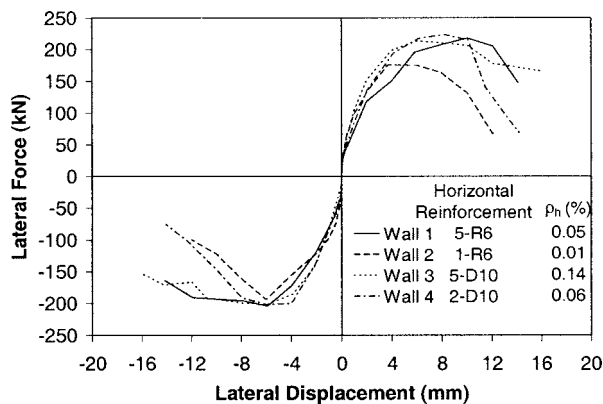


Fig. 6. Effect of shear reinforcement on masonry shear strength

to satisfy the requirements of continuity of shear flow and to avoid the possibility of vertical shear failure up a continuous ungrouted flue. This resulted in an effective width of 60 mm for the partially grout-filled concrete masonry walls. The F_n value included in Table 2 was the lateral force required to develop the nominal flexural strength of the wall and was evaluated based on a rectangular masonry compression stress block using measured rather than specified material strengths.

Fig. 4 depicts a selection of experimentally obtained force-displacement curves. The force corresponding to the wall nominal flexural strength is identified by the symbol F_n . Also shown on these plots are lines corresponding to the predicted shear strengths derived from Eq. (1) (denoted NZS4230) and Eq. (2) [denoted National Earthquake Hazards Reduction Program (NEHRP)]. Table 2 and Fig. 4 both show that for all walls (except Wall 3), the predicted shear strength was less than the force corresponding to the predicted flexural strength.

All walls, except for Walls 1 and 3, exhibited shear dominated response. This type of response was characterized by the development of early horizontal flexural cracks that were then superceded by wide-open diagonal cracks that extended throughout the masonry walls. These diagonal cracks were initiated by tension splitting of masonry in the compression strut that formed in the walls. Rapid strength degradation was observed for walls that failed in the shear dominated mode [see Figs. 4(c and d)], attributed to the widening of diagonal cracks and crushing of masonry.

Although Wall 1 was expected to fail in shear, it did not exhibit sudden strength degradation after reaching maximum wall strength, therefore indicating possible yielding of vertical rein-

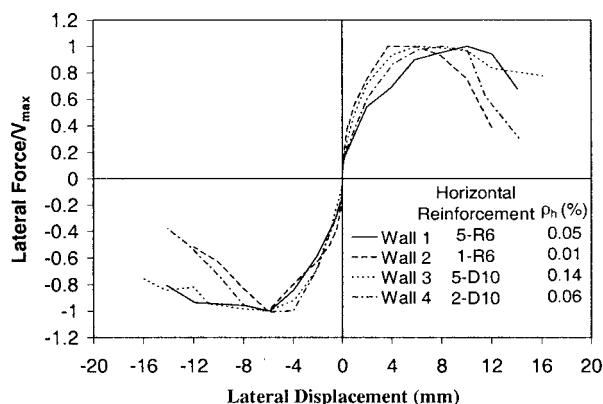


Fig. 7. Force-displacement envelopes normalized with V_{max}

forcement during testing. Consequently, it was classified as having a flexure/shear type of failure. This type of failure mode was possible due to the absence of axial load and the adoption of closely distributed shear reinforcement using small size reinforcing bars (i.e., R6). Accordingly, the initial diagonal cracks did not widen significantly under increasing lateral force, but instead new sets of diagonal cracks formed and gradually spread over the wall diagonals, accompanied by higher energy dissipation and ductile behavior. It is also shown in Fig. 4(b) that Wall 3 failed to reach F_n . This was due to significant sliding at the wall base. Consequently, a portion of the shear force was transferred by dowel action of vertical reinforcement. This in turn led to a reduction in wall lateral strength. Fig. 5 illustrates wall cracking patterns at the end of testing. The shaded areas shown in Fig. 5 indicate masonry crushing.

The data of Fig. 4 confirm that the NZS 4230:1990 shear expression significantly underpredicted the in-plane shear strength of masonry walls. It is also observed from the same figure that shear prediction using Eq. (2) provided a better match for walls that had $H_e/L \leq 1.0$. However, Fig. 4(f) illustrates that Eq. (2) overpredicted the shear strength of Wall 9 by about 23%. This overprediction of shear strength was due to the substantial increase in diagonal shear cracking (compared to other walls) that developed before the maximum wall strength was reached, and also due to the fact that Eq. (2) does not address the reduction in masonry shear strength within potential plastic hinge regions. Experimental results indicated that a displacement ductility level of 2.9 was recorded when Wall 9 developed its maximum strength.

Discussion

This section discusses how design parameters, such as the amount of shear reinforcement, distribution of shear reinforcement, magnitude of axial compression load, wall H_e/L ratio, and type of grouting affect the shear strength of masonry walls. The figures in this section are limited to force-displacement envelopes, arranged in groups to show the effect of a particular parameter.

Effect of Shear Reinforcement

In this study both the amount of shear reinforcement and the distribution of reinforcing bars throughout the height of the wall were varied. It was observed that a change in the quantity of shear reinforcement had a direct influence on V_n . This is clearly illustrated in the experimental results shown in Fig. 6, where the maximum shear strength increased from 195 kN for Wall 2 to 215 kN for Wall 1, resulting in a strength increase of 10% when the shear reinforcement increased from 1 R6 to 5 R6 reinforcing bars.

Fig. 7 shows the effectiveness of horizontal reinforcement in enhancing the post-cracking performance of masonry walls. It can be seen that the deformability of walls improved when the amount of shear reinforcement increased from 1 R6 to 5 R6 reinforcing bars for the case of Walls 2 and 1, and when the horizontal reinforcement increased from 2 D10 to 5 D10 reinforcing bars for the case of Walls 4 and 3. The advantage of distributing shear reinforcement (using a greater number of reinforcing bars of smaller diameter) up the height of the wall can be clearly observed by comparing the force-displacement envelopes of Walls 1 and 4. The two walls contained approximately the same total cross-sectional area of shear reinforcement, but the shear reinforcement was distributed differently. Fig. 7 shows that Wall 4

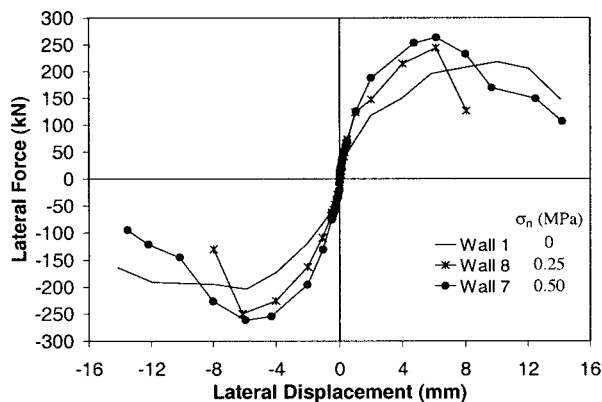


Fig. 8. Effect of axial compression stress on masonry shear strength

exhibited abrupt strength degradation after the peak wall strength was attained, whereas Wall 1 exhibited a more gradual strength degradation. This type of failure was made possible for Wall 1 due to the adoption of 400-mm spaced horizontal reinforcement. The closely spaced shear reinforcement enabled the distribution of stresses throughout the wall diagonals after the initiation of shear cracking. Accordingly the initial diagonal cracks did not widen significantly under increasing lateral displacements; instead, new sets of diagonal cracks formed and gradually spread over the wall diagonals, accompanied by higher energy dissipation and more ductile behavior. It was therefore possible to classify Wall 1 as having a flexure/shear type of failure or “ductile shear failure.” Conversely, Wall 4 exhibited a “brittle shear failure.” This type of shear failure was expected since Wall 4 was constructed without the closely distributed shear reinforcement. This prevented the tensile stress due to applied shear force from being adequately transferred across the diagonal cracks. Hence, the cracks opened extensively, resulting in a major x-shaped diagonal crack pair [see Fig. 5(d) for wall crack pattern], leading to a relatively sudden and destructive failure.

Effect of Axial Compression Stresses

The positive influence of axial compression stress on masonry shear strength is illustrated in Fig. 8. This figure shows the performance of the three masonry walls that had the same dimensions and reinforcement details, but were subjected to varying levels of axial compression stress. The maximum shear strength increased from 215 kN (Wall 1), to 244 kN (Wall 8) and 263 kN

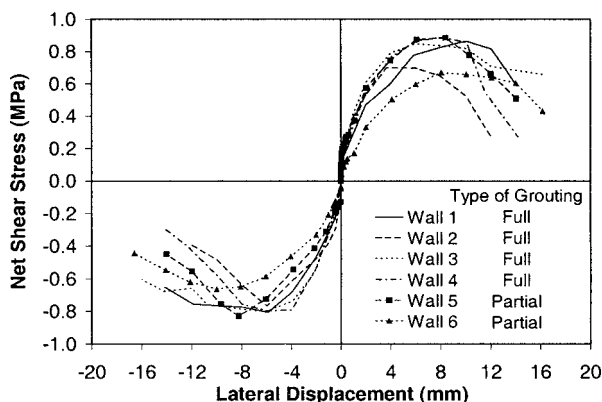


Fig. 9. Effect of grouting on masonry

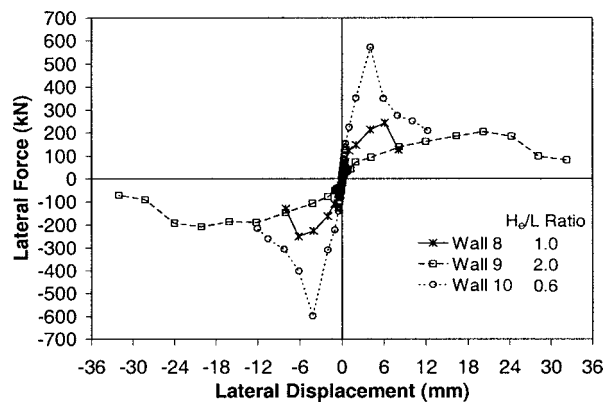


Fig. 10. Effect of H_e/L on masonry shear strength

(Wall 7) when the axial compression stress was increased from zero to 0.25 MPa and 0.50 MPa, resulting in an increase of about 13% and 22%, respectively. Also observed from the same figure is reduction of the postcracking deformation capacity of Walls 7 and 8. This was because the failure type became more brittle as the axial compression stress increased.

It was also noted from observations made during the experimental process that an increase in axial compression stress delayed the initiation of cracking until larger lateral force was applied. This can be explained from principal stresses: a larger lateral force is required to exceed the compressive field resulting from the larger axial load. This compressive field must first be overcome before cracking can initiate.

Effect of Grouting

Experimental results presented in Table 2 illustrate the significant reduction of shear strength when the masonry walls were partially grouted. For the partially grouted masonry walls, it was also shown that Wall 5, with five grouted flues, had about 50% higher strength than the corresponding Wall 6, which had only three grouted flues. However, the effect of grouting method becomes less significant when the net shear stress is calculated by considering the cross-sectional area of both the CMUs and the grouted cells. This is shown in Fig. 9, where force-displacement envelopes of both fully (without axial load) and partially grouted walls (Walls 5 and 6) are presented.

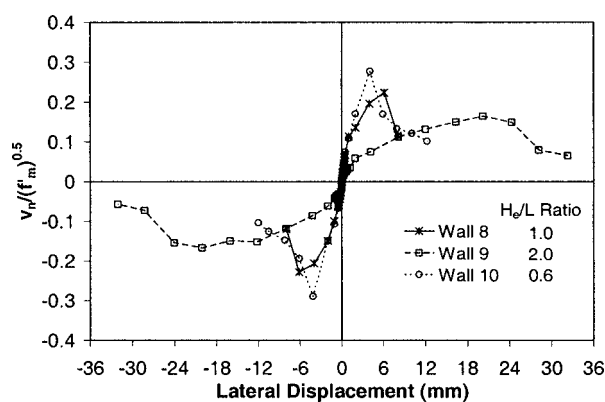


Fig. 11. Relationship of $v_n / \sqrt{f'_m}$ versus H_e/L

Effect of Wall H_e/L Ratio

Fig. 10 illustrates that the masonry shear strength decreased from a maximum of 244 kN for Wall 8 ($H_e/L=1.0$) to 207 kN when the H_e/L ratio was increased to 2.0 in the case of Wall 9, resulting in a decrease of 15%. Fig. 10 also shows a significant increase in masonry shear strength for Wall 10 that was constructed to a reduced H_e/L ratio. This indicates that masonry shear strength increases as the H_e/L ratio decreases, while it decreases inversely in relation to an increase in the H_e/L ratio. It is realized, however, that the different shear strengths shown in Fig. 10 could have been due to the variations in the net area A_n and in f'_m . In order to meaningfully observe the relation between masonry shear strength and H_e/L ratio, the influence of A_n and f'_m must be excluded from the test results. Consequently, a plot of $v_n/\sqrt{f'_m}$ is presented in Fig. 11. As anticipated, tendency similar to that observed in Fig. 10 is evident.

Conclusions

The effects of shear reinforcement, axial compression load, type of grouting, and wall aspect ratio on masonry shear strength were investigated in this study. It was established that axial compression load had a significant influence on the in-plane shear performance of masonry shear walls, mainly because it suppressed the tensile field in a material inherently weak in tension. Consequently, as the axial compression load increased, so did the ability of the walls to provide shear resistance. However, the postcracking deformation capacities were observed to reduce with increasing axial load. This was because of the increasing brittleness of this failure type as the axial compression stress increased.

It was observed that shear reinforcement not only provided additional shear resistance, but also improved the postcracking performance of the masonry walls when shear reinforcement was uniformly distributed up the height of the walls. The provision of closely spaced shear reinforcement enabled the distribution of stresses throughout the wall diagonals after the initiation of shear cracking. Accordingly, the initial diagonal cracks did not widen significantly under increasing lateral displacements, but instead new sets of diagonal cracks formed and gradually spread over the wall diagonals, accompanied by higher energy dissipation and more ductile behavior. The test results also demonstrated that partial grouting significantly reduced masonry shear strength. However, the effect of grouting became less significant when net shear stress was calculated accounting for the cross-sectional area of both the masonry units and grouted cells. In addition, the test results indicated that masonry shear strength decreased inversely in relation to the H_e/L ratio.

Finally, the test results demonstrated that NZS 4230:1990 was conservative in its treatment of masonry shear strength. This was shown by the constant underprediction of shear strength for the masonry walls investigated in this study. The test results of this study also demonstrated that the NEHRP masonry shear expressions provided reasonably accurate prediction for walls that had $H_e/L \leq 1.0$, but overpredicted the shear strength of Wall 9 that had $H_e/L=2.0$.

Acknowledgments

This research was funded by the Earthquake Commission Research Foundation (EQC). Materials and construction labor asso-

ciated with the testing of masonry walls was provided by Firth Industries Ltd., W. Stevenson and Sons Ltd., and Ready Mix Concrete Ltd. Their contributions are gratefully acknowledged. The authors also wish to acknowledge contributions by Hank Mooy and Tony Daligan, who were responsible for the practical aspects in relation to testing of the wall specimens in the Civil Test Hall of the University of Auckland.

The opinions and conclusions presented herein are those of the authors, and do not necessarily reflect those of the University of Auckland or any of the sponsoring parties to this project.

Notation

The following symbols are used in this paper:

- A_n = net cross-sectional area of wall;
- d_u = lateral displacement at wall failure;
- d_{vmax} = displacement at maximum recorded lateral force;
- F_n = lateral force to generate calculated wall nominal flexural strength;
- f'_m = masonry compressive strength;
- f_{yh} = yield strength of horizontal shear reinforcement;
- H = wall height;
- H_e = effective wall height;
- L = wall length;
- V_{max} = experimentally recorded maximum lateral force;
- V_n = nominal shear strength of masonry wall;
- v_m = permissible shear stress;
- ρ_h = shear reinforcement ratio; and
- σ_n = axial compressive stress.

References

- Chen, Shi-Wen J., Hidalgo, P. A., Mayes, R. L., Clough, R. W., and McNiven, H. D. (1978). "Cyclic loading tests of masonry single piers, vol. 2: Height to width ratio of 1." *Report No. UCB/EERC-78/28*, Earthquake Engineering Research Center, Univ. of California, Berkeley, Calif.
- Hidalgo, P. A., Mayes, R. L., McNiven, H. D., and Clough, R. W. (1979). "Cyclic loading tests of masonry single piers. Vol. 3: Height to width ratio of 0.5." *Report No. UCB/EERC-79/12*, Earthquake Engineering Research Center, Univ. of California, Berkeley, Calif.
- Hiraishi, H. (1985). "Flexural behaviour of reinforced masonry walls." *Proc., 1st Meeting of the U.S.-Japan Joint Technical Coordinating Committee on Masonry Research*, Tokyo.
- Matsumura, A. (1988). "Shear strength of reinforced masonry walls." *Proc., 9th World Conf. on Earthquake Engineering*, Vol. 7, 121–126.
- Mayes, R. L., Omote, Y., and Clough, R. W. (1976). "Cyclic shear tests on masonry piers. Vol. 1: Test results." *Report No. UCB/EERC-76/8*, Earthquake Engineering Research Center, Univ. of California, Berkeley, Calif.
- National Earthquake Hazards Reduction Program (NEHRP). (1997). "Recommended provisions for seismic regulations for new buildings and other structures. Part 1: Provisions." *Building Seismic Safety Council*, Washington, D.C.
- Priestley, M. J. N. (1977). "Seismic resistance of reinforced concrete masonry shear walls with high steel percentages." *Bulletin of the New Zealand National Society for Earthquake Engineering*, 10(1), 1–16.
- Priestley, M. J. N. (1980). "Seismic design of masonry buildings—background to the draft masonry design code DZ 4210." *Bulletin of the New Zealand National Society for Earthquake Engineering*, 13(4),

- Shing, P. B., Schuller, M., and Hoskere, V. S. (1990). "In-plane resistance of reinforced masonry shear walls." *J. Struct. Eng.*, 116(3), 619–640.
- Sveinsson, B. I., Mayes, R. L., and McNiven, H. D. (1985). "Cyclic loading of masonry single piers. Vol. 4: Additional test with Height to Width Ratio of 1." *Report No. UCB/EERC-85/15*, Earthquake Engineering Research Center, Univ. of California, Berkeley, Calif.
- Voon, K. C., and Ingham, J. M. (2001). "Toward suitable shear strength provisions for inclusion in the New Zealand masonry design standard." *Proc., 6th Australasian Masonry Conference*, Adelaide, South Australia, 393–402.
- Voon, K. C., and Ingham, J. M. (2003). "Shear strength of concrete masonry walls." *School of Engineering Report No. 611*, Univ. of Auckland, Auckland, New Zealand.

Experimental In-Plane Strength Investigation of Reinforced Concrete Masonry Walls with Openings

K. C. Voon¹ and J. M. Ingham, M.ASCE²

Abstract: This paper presents test results of eight partially grout-filled perforated concrete masonry walls that were subjected to cyclic lateral loading. Test results obtained from this research indicated that the size of openings and the length of trimming reinforcement significantly affected the lateral strength of perforated masonry walls. It was shown that the current New Zealand nonspecific masonry design standard NZS 4229 unsafely overpredicts the strength capacity of concrete masonry walls with small openings, and an amendment is proposed to rectify this matter. It was also shown that NZS 4229 is increasingly conservative as the height of openings increased. Diagonal cracking patterns that formed during testing were observed to align well with the load paths by which lateral shear force was assumed to be transferred to the foundation when using strut-and-tie analysis. This observation supports the use of the strut-and-tie technique as a viable tool to evaluate the flexural strength of walls of this type.

DOI: 10.1061/(ASCE)0733-9445(2008)134:5(758)

CE Database subject headings: Concrete masonry; Walls; Grouting; Openings; Reinforcement; Cyclic load.

Introduction

For many decades, masonry has been used as a common structural material in a large proportion of New Zealand building projects. However, the poor performance of unreinforced masonry in the magnitude 7.8 1931 Hawke's Bay earthquake (Dowrick 1998; Scott 1999) subsequently led to a ban on all unreinforced masonry in New Zealand, and the associated development of conservative reinforced concrete masonry design provisions. Consequently, a typical detail in fully-grouted concrete masonry walls was the use of \varnothing 12 mm deformed reinforcing bars having a characteristic yield strength of 300 MPa and spaced at 400 mm centers, both vertically and horizontally. The recent promulgation of alternative construction forms such as tilt-up precast concrete wall systems has resulted in the perception within New Zealand that reinforced concrete masonry is an expensive form of construction when compared with competing products and systems. Consequently, a decision was made by the New Zealand concrete masonry industry to develop a nonspecific design standard NZS 4229 (NZS 1999) which, while retaining suitable conservatism, was more realistic in its treatment of measured

experimental response. In particular, it was permitted to use partially grout-filled nominally reinforced concrete masonry in the most seismically active regions of New Zealand. Furthermore, efforts were made to simplify use of the standard so that the design of single and double story masonry structures, not containing crowds and not dedicated to the preservation of human life, could be effectively conducted by architects and architectural draftspersons with limited, if any, input from consulting structural engineers.

The in-plane lateral strength of a masonry panel is specified in NZS 4229 through determination of its "bracing capacity," with the bracing capacity values being derived from wall tests conducted at the University of Auckland by Brammer (1995) and Davidson (1996), of which only two considered the performance of walls with openings. However, it was subsequently identified that an important lintel reinforcement detail adopted in testing of these two walls differed from that specified in NZS 4229. Hence, a third wall, having an opening and with reinforcement detailing complying with NZS 4229 was tested (Ingham et al. 2001), and it was observed that this wall did not achieve the bracing capacity prescribed in NZS 4229. Further assessment indicated that the existing design standard may be nonconservative in its treatment of walls with openings. Consequently, an experimental study was conducted at the University of Auckland to investigate the influence of openings in partially grout-filled nominally reinforced concrete masonry walls.

This paper describes the results from structural testing of eight single story-height concrete masonry walls that were recently reported in comprehensive form in Voon and Ingham (2006). The primary objective of the study was to validate the adequacy of NZS 4229 in addressing the bracing capacity of masonry walls containing openings. The eight walls of the study had variations in lintel reinforcement detailing, including detailing that complied with NZS 4229 and a range of penetration geometries.

¹Formerly, Ph.D. Student, Dept. of Civil and Environmental Engineering, Univ. of Auckland, Private Bag 92019, Auckland, New Zealand. E-mail: kcvoon@yahoo.com

²Associate Professor, Dept. of Civil and Environmental Engineering, Univ. of Auckland, Private Bag 92019, Auckland, New Zealand. E-mail: j.ingham@auckland.ac.nz

Note. Associate Editor: Li Bing. Discussion open until October 1, 2008. Separate discussions must be submitted for individual papers. To extend the closing date by one month, a written request must be filed with the ASCE Managing Editor. The manuscript for this paper was submitted for review and possible publication on March 12, 2007; approved on October 8, 2007. This paper is part of the *Journal of Structural Engineering*, Vol. 134, No. 5, May 1, 2008. ©ASCE, ISSN 0733-9445/2008/5-758-768/\$25.00.

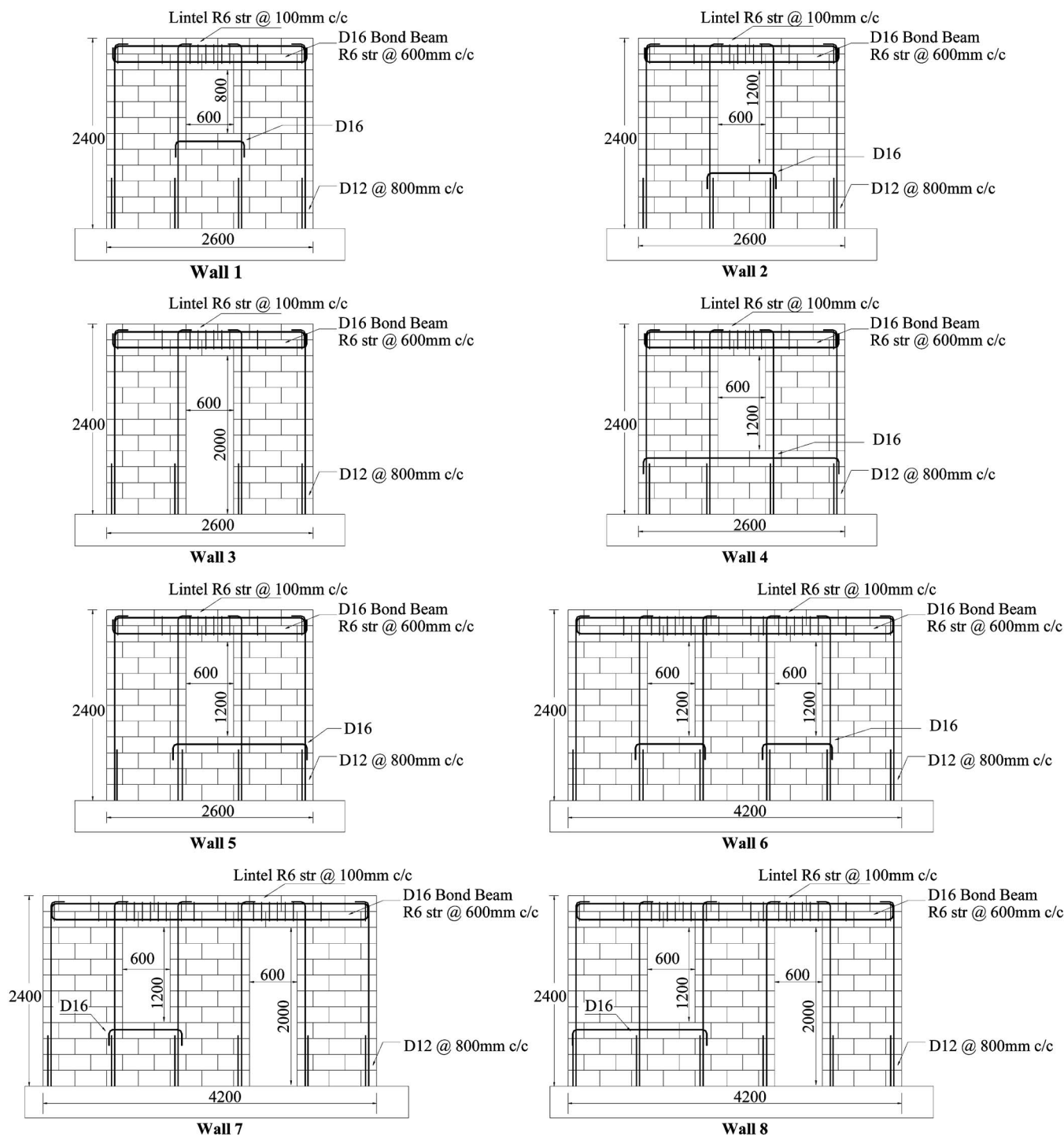


Fig. 1. Wall geometries and reinforcing details

Experimental Program

Test Specimens

The geometries and reinforcement details of the eight single-story masonry walls are shown in Fig. 1. All eight walls were partially grout filled, where only those cells containing reinforcement were grouted, and were constructed to a common height of 2,400 mm. None of the eight masonry walls had applied axial compression load. The vertical reinforcement of the partially grout-filled walls

shown in Fig. 1 was spaced at 800 mm centers, and the horizontal reinforcement in all walls consisted of two D16 reinforcing bars placed in a solid grout-filled bond beam within the top two block courses and a D16 trimming reinforcing bar placed below all window openings. All wall openings had a length of 600 mm.

All walls were constructed by experienced masons under supervision, and employed a running bond pattern of standard production 15 series (140 mm wide) precast concrete masonry units (CMUs). The mortar used throughout the study was a preblended bagged 1:4 mix of portland cement to sand by volume. High

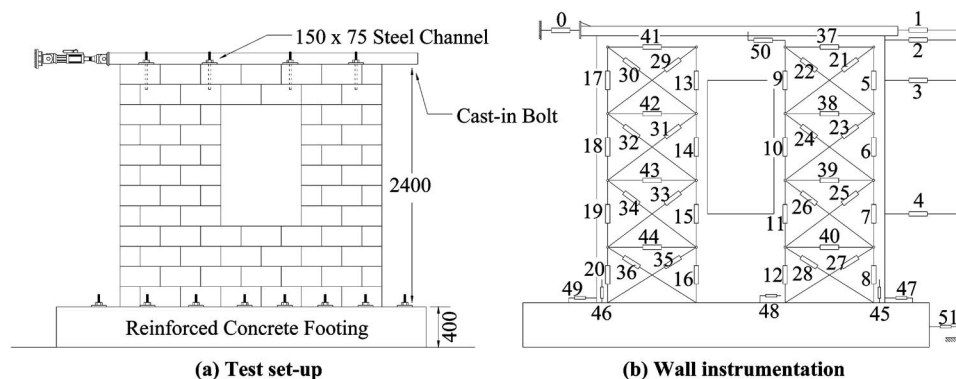


Fig. 2. Typical test setup and wall instrumentation

slump ready-mix grout using small aggregate (7 mm) was employed for filling the cavities within the test walls and a common commercially used expansive chemical additive was added to the grout to avoid formation of voids caused by high shrinkage of the grout.

Test Setup and Instrumentation

The testing of specimens reported herein was conducted according to the setup shown in Fig. 2(a). The test setup and method of loading adopted in this experimental program were designed to simulate the response that a masonry shear wall would experience during seismic excitation. Although a single-story wall does not have the complexity of a multistory structure, it is advantageous to consider due to the ease of data interpretation. Horizontal cyclic loading was applied to the top of the wall via a 150×75 steel channel as shown in Fig. 2(a), which was fastened to the top of the bond beam by cast-in bolts. The jack was fastened to the strong wall, and the tested wall was stabilized from moving in its out-of-plane direction by two parallel horizontal struts, which were positioned perpendicular to the wall and hinged to the channel and a reaction frame. Fig. 2(b) schematically shows typical wall instrumentation. A load cell to measure the magnitude of the lateral force was placed between the actuator and the steel channel, denoted as device 0 in Fig. 2(b). Portal displacement transducers, denoted as 1 and 2, measured lateral displacement at the top of the wall. Displacements at the window levels were measured by instruments 3 and 4. Portal displacement transducers 47–49 were used to measure sliding of the wall relative to the concrete footing, and transducers 45 and 46 measured the uplift at wall toe positions. Any slip in the steel channel and the concrete footing were measured by transducers 50 and 51, respectively. Further transducers were placed according to the configuration shown in Fig. 2(b) to attain the shear and flexural components of deformation.

Material Properties

Samples were taken from steel reinforcement used in wall construction. These samples were subjected to tensile testing, with the average yield strengths (f_y) for the D12 and D16 reinforcing steel being 305 and 315 MPa, respectively. In addition, masonry compression strength f'_m was determined by material testing of masonry prisms. These prisms were built of three concrete masonry units stacked on top of each other, using the same construction technique as was used for the wall. The prisms were grout filled at the same time as the wall, and were then subjected to the

same curing condition as the wall panels. The prisms were tested using an Avery universal testing machine, with f'_m values summarized in Table 1.

Wall Strength Prediction

NZS 4229 Codification of Wall Capacity

NZS 4229 is primarily intended for use by architects and draftspersons, rather than structural engineers. Consequently, a simplified procedure was adopted for the assessment of bracing capacity. The strategy employed in NZS 4229 for proportioning bracing capacity is primarily dependent on wall geometry. The assumption was that the bracing capacity of a masonry wall having penetrations could be determined based on the geometry of individual bracing panels, as demonstrated by the shaded areas shown in Fig. 3, where the geometry of each bracing panel is based upon the vertical dimension of the smallest adjacent opening. The total bracing capacity is then assumed to be the sum of the capacities provided by the individual bracing panels of the wall. The evaluated wall strengths using the NZS 4229 procedure are identified as F_{code} in Table 1. From Table 2, it is evident that for a given panel, the bracing capacity increases as the panel length increases, but diminishes as the panel height increases. This prompted some observers to comment on the influence that a small wall opening would have, as this would effectively generate two bracing panels with a small height and located at either side of the opening, rather than the wall being considered as a single panel that is taller and longer. It was then conceivable that the addition of a small opening to the wall might result in the illogical result that the evaluated capacity of the wall increased.

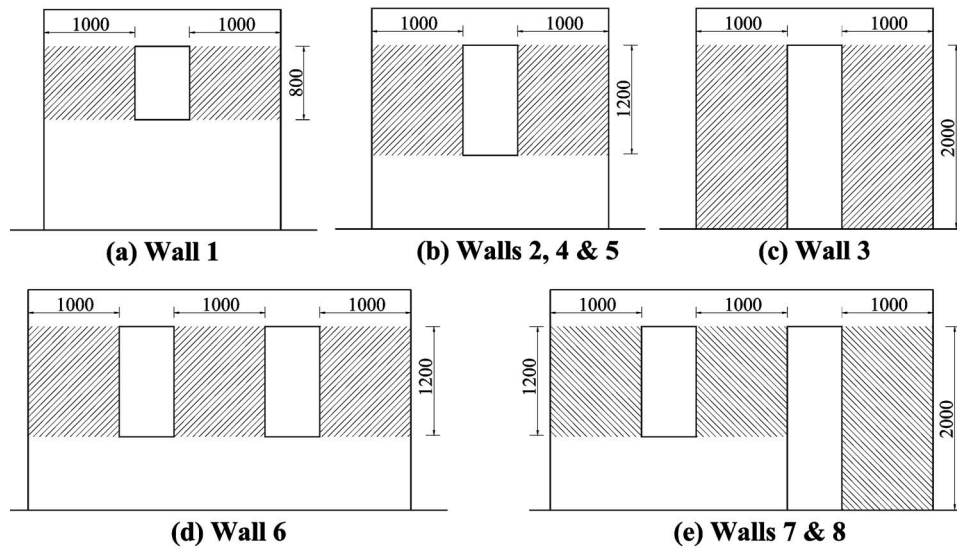
Prior to testing, the flexural strengths of the masonry walls were evaluated using the bracing capacity values specified in NZS 4229, with the relevant information reproduced in Table 2 for partially grouted 15 series (140 mm thick) concrete masonry. These bracing values were derived by assuming a reinforcement lower characteristic yield stress of $f_y=300$ MPa and a masonry characteristic compression strength of $f'_m=8$ MPa, and by treating the panels as vertical flexural cantilevers with a height measured to the center of the fully grouted bond beam. It is emphasized that the conservatism of these NZS 4229 bracing capacities with respect to the experimental results (Brammer 1995; Davidson 1996) was primarily attributed to the actual material strengths being significantly greater than specified, the adoption of a flexural strength reduction factor of $\phi=0.8$, and a further reduction to

Table 1. Summary of Wall Behavior

Wall number	L_w	h_{op}/h_w	f'_m	F_{code}	$F_{n,st0}$	$F_{n,st1}$	F_{max}	Δ_y	μ_{max}	μ_{ev}	$\frac{F_{max}}{F_{n,st0}}$	$\frac{F_{max}}{F_{n,st1}}$	$\frac{F_{max}}{F_{code}}$	$\frac{F_{max}}{F_{code}^*}$
1	2,600	0.33	16.2	51.8	44.7	46.4	+50.2 -49.0	0.82	+6 -4	>6.0	1.12 1.10	1.08 1.06	0.97 0.95	1.21 1.18
2	2,600	0.5	12.9	37.3	35.9	38.4	+41.2 -38.7	0.57	± 4	>6.0	1.15 1.08	1.07 1.00	1.11 1.04	1.23 1.15
3	2,600	0.83	14.4	24.3	28.0	30.8	+33.3 -34.4	1.07	± 4	>6.0	1.19 1.23	1.08 1.12	1.37 1.42	1.37 1.42
4	2,600	0.5	16.5	37.3	41.0	44.7	+47.4 -48.8	1.15	+2 -4	4.5	1.16 1.19	1.06 1.09	1.27 1.31	1.27 1.31
5	2,600	0.5	18.9	37.3	41.0	44.7	+52.4 -35.9 -38.4 -50.4	+0.84 -0.66	+4 -6	2.0	1.28 1.40	1.17 1.31	1.40 1.35	1.40 1.35
6	4,200	0.5	16.5	55.9	58.0	78.3	+94.3 -94.6	1.83	+2 -4	2.0	1.63	1.20	1.69	1.69
7	4,200	0.83 ^a	18.0	49.4	50.0	62.1	+82.8 -73.0 -82.5	1.89	± 4	3.8	1.66 1.13	1.33	1.68	1.68
8	4,200	0.83 ^a	18.0	49.4	50.0	62.1	+82.7 -55.0 -76.3 -93.2	1.60	± 4	2.0	1.66 1.69	1.33 1.22	1.89	1.89
B1	2,600	0	—	46.0	—	75.0	76.5	1.57	—	5.4	—	1.02	1.66	1.66
B2	4,200	0	—	85.6	—	213.1	179.9	3.60	—	1.0	—	0.84	2.10	2.10
Units	mm	—	MPa	kN	kN	kN	kN	mm	—	—	—	—	—	—

Note: h_{op}/h_w ratio according to the largest opening on the wall; Walls B1 and B2 were tested by Brammer (1995); + denotes push loading; - denotes pull loading.

^aRefers to magnitude of largest opening.

**Fig. 3.** Identification of bracing panels**Table 2.** Bracing Capacities (kN) for 140 mm Partially Grouted Concrete Masonry (from NZS 4229)

Panel height (m)	Panel length (m)								
	0.8	1.2	1.6	2.0	2.8	3.6	4.4	5.2	6.0
0.8	19.3	32.5	50.3	71.3	125.3	155.5	222.8	302.0	393.5
1.2	13.8	23.5	36.5	51.8	91.3	113.3	162.5	220.8	287.5
2.0	9.0	15.3	24.0	34.0	60.3	75.0	107.8	146.5	191.3
3.0	6.3	10.8	17.0	24.5	43.5	54.3	78.0	106.3	139.0

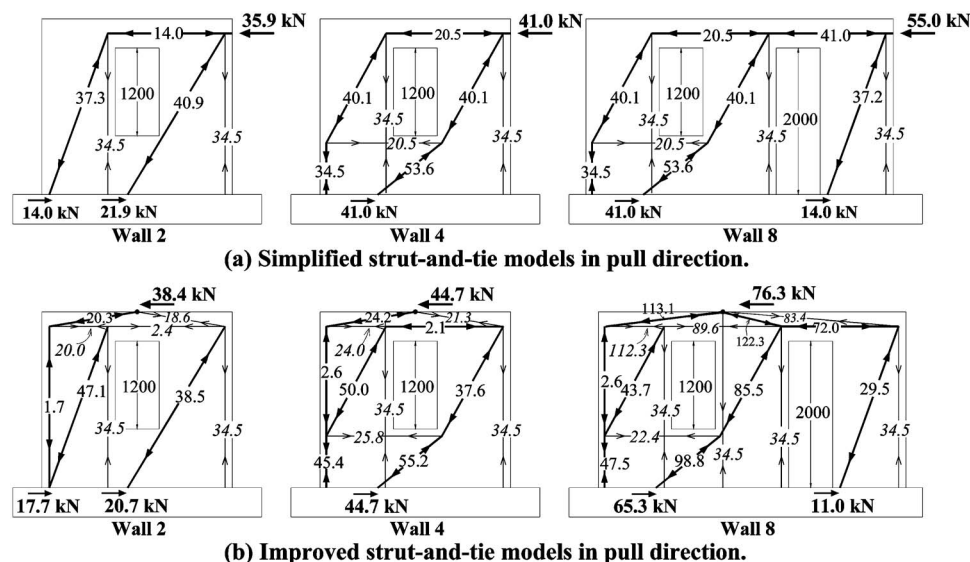


Fig. 4. Wall strength analysis models

80% of the evaluated capacity for panels having a length greater than 3.0 m. In addition, in all cases the calculation assumed the vertical \varnothing 12 mm reinforcement to be distributed at a maximum spacing of 800 mm (where possible) or for bars to be spaced in the least favorable positions, resulting in the most conservative estimate of flexural strength.

Simple Strut-and-Tie Models

Two types of strut-and-tie models were employed to evaluate wall strengths (Yanez et al. 1991; Wu and Li 2003). The first type was a simplified strut-and-tie model, which assumed that all panels were pinned at the bond beam center and that lateral force was applied to the bracing panels at the center of the bond beam. These assumptions corresponded directly with those assumed in NZS 4229. In addition, the effect of wall self-weights was not considered in this simplified strut-and-tie model in order to ease the analysis process. The resultant strut-and-tie analyses using this simplified procedure are diagrammatically shown in Fig. 4(a) for a selection of walls loaded in the pull direction, where the strut components are indicated by a broader element thickness. It is illustrated in Fig. 4(a) that the introduction of extended trimming reinforcement beneath the window in Wall 4 results in an increase in wall strength when compared to that predicted for Wall 2. This is due to the change of slope of the diagonal strut in the left panel of Wall 4. The evaluated lateral wall strengths using this simplified strut-and-tie analysis procedure are identified as $F_{n,st0}$ in Table 1.

Improved Strut-and-Tie Models

A second set of strut-and-tie models considered the lateral force to be applied as a single point load at the center of the wall top, which more accurately represented the loading system shown in Fig. 2(a). These models are referred to here as “improved” to clearly delineate them from the “simple” models previously discussed. The lateral force was transferred from the wall top to the bond beam center through a triangular truss, which was subsequently applied to the bracing panels. Unlike the simplified models presented in Fig. 4(a), the wall self-weight of 1.6 kN/m² was

considered to act along the bond beam center in the improved strut-and-tie models. The resultant strut-and-tie analyses using the above mentioned procedure are diagrammatically shown in Fig. 4(b) for pull direction loading.

Similar to the simplified strut-and-tie analysis procedure discussed earlier, an increase in predicted strength is illustrated in Fig. 4(b) when extended trimming reinforcement is included in Wall 4. The predicted lateral wall strengths using the improved strut-and-tie models are identified as $F_{n,st1}$ in Table 1, where it is shown that the improved modeling procedure resulted in predicted strength increases of between 4 and 10% for the 2.6 m long perforated masonry walls. For the 4.2 m long walls with two openings, where double bending of the central pier was also modeled in the improved strut-and-tie formulation, the predicted strength increased by 23 to 52%.

Shear Strength

Wall shear strength was evaluated using the NZS 4230 (NZS 2004) procedure (Voon and Ingham 2007) and was found to be substantially in excess of the lateral force required to generate the nominal flexural strength.

Experimental Results

General wall behavior is summarized in Table 1, where F_{max} corresponds to the maximum wall strength measured in the test, and Δ_y is the evaluated yield displacement of the tested walls. μ_{max} is defined as the displacement ductility level at which maximum strength was measured and μ_{av} is the experimentally determined available displacement ductility factor. It is important to note that NZS 4229 assumes maximum seismic demands and capacities based upon a maximum displacement ductility of $\mu=2$ (Ingham et al. 2001). Consequently, wall response exceeding $\mu=2$ represents superior wall response and correspondingly conservative seismic design.

The experimentally obtained force-displacement curves for masonry walls are presented in Fig. 5, depicting the lateral dis-

placement at the top of the walls as a function of applied lateral shear force. Due to the lack of horizontal shear reinforcement and the fact that the walls were partially grout filled, all test walls were observed to fail in a diagonal tension mode. The general nature of the force-displacement responses presented in Fig. 5 are notably similar to those reported by Brammer (1995) and Davidson (1996). From the force-displacement histories illustrated in Fig. 5, a number of general characteristics of the masonry walls can be identified:

1. The maximum strength was typically developed during the first excursion to $\mu=4$. Following this, cracking became significant in some walls and strength degradation began.
2. Despite the presence of widely open diagonal cracks, the partially grouted walls exhibited only gradual strength and stiffness degradation, and in no case did any wall suffer from sudden failure. This desirable behavior of the nominally reinforced partially grouted masonry walls with openings was due to the solid filled bond beam at the top of the walls, which caused a frame-type action at a later stage of testing.
3. The force-displacement plots consistently illustrated a pinched shape. This was primarily due to the presence of significant shear deformation in this type of masonry construction. Less hysteretic energy was expended during the second cycle to any displacement level, when compared with the first displacement cycle. This is illustrated by the more pinched hysteresis loops of the second cycle.
4. From the wall cracking patterns diagrammatically shown in Fig. 6, it is clearly illustrated that the absence of major damage in the solid grout-filled bond beam supported the notion of frame-type action being developed at a later stage of testing. This led to considerable inelastic displacement capacity of the partially grouted masonry walls, where μ_{av} was measured to consistently be above 2.0.

The μ_{av} values recorded in Table 1 show that the largest recorded ductility capacity for the perforated masonry walls corresponded to a wall length of 2,600 mm, and reduced significantly for the 4,200 mm long perforated masonry walls. It was observed during experimental testing that the 4,200 mm long masonry walls displayed greater cracking than the 2,600 mm long walls. Consequently, it was deduced that the lower observed ductility rating for the 4,200 mm long walls occurred because of the rapid-developing wide cracks that contribute to shear displacement, accelerating initiation of the diagonal tension mode of failure and subsequent strength degradation.

From Fig. 5(a), it was observed that Wall 1 did not achieve the bracing capacity prescribed by NZS 4229 (denoted F_{code}). NZS 4229 overpredicted the lateral strength of this perforated wall by about 3.3 and 5.4% in the respective push and pull directions. However, it is illustrated in Fig. 5 that the conservatism of NZS 4229 increases with the height of opening, and for a full height opening (e.g., a door in Wall 3) the NZS 4229 prediction had significant conservatism. Consequently, it was concluded that NZS 4229 is only nonconservative for window openings having a height of less than 1.2 m, though unfortunately this probably accounts for a significant proportion of window geometries.

Due to the lack of distributed horizontal shear reinforcement and the fact that the wall was partially grout filled, all test walls were observed to fail in diagonal tension mode. This type of failure was characterized by the development of early horizontal flexural cracking, which was later superseded by wide diagonal cracks that extended throughout the wall panels. The cracking patterns for these walls are depicted diagrammatically in Fig. 6, with the shaded areas indicating masonry crushing. From Fig. 6 it

may be observed that the diagonal cracking patterns on the perforated concrete masonry walls aligned well with the load paths by which shear force was transferred to the foundation in the strut mechanisms of Fig. 4.

Discussion

The primary objective of this study was to validate the adequacy of NZS 4229 in addressing the bracing capacity of masonry walls containing openings. As shown in Fig. 1, design of the perforated masonry wall specimens was conceived to facilitate comparison of wall behavior between two or more walls with respect to variation of a given dimension of wall geometry.

Height of Openings

Test results successfully illustrated correlation between the reduction of wall strength and the increasing height of wall openings (h_{op}). This reduction of wall strength is also identified in the force-displacement envelopes presented in Figs. 7 and 8. In Fig. 7, it is shown that the lateral strength of the 2,600 mm long walls reduced from the maximum of 76.5 kN in the case of Wall B1 without an opening [reported by Brammer (1995)], to 50.2 kN when a window opening of 600×800 was included in Wall 1. The same figure also shows further reduction of wall strength to 41.2 kN and 34.4 kN when the height of openings was increased to 1,200 mm and 2,000 mm in Walls 2 and 3, respectively. As diagrammatically illustrated in the pull direction strut-and-tie models presented in Fig. 9, the further reduction of strength in Walls 2 and 3 (compared to Wall 1) was because of the more steeply inclined diagonal strut of the right piers as the height of openings increased. This resulted in a reduction of the horizontal shear component that could be resisted by the right pier, consequently leading to the overall reduction of lateral strength in Walls 2 and 3.

Similarly, the reduction of lateral strength in the 4,200 mm long walls is evident in Fig. 8. As compared to the strength recorded in Wall B2 [reported by Brammer (1995)], it is shown that the wall lateral strength was almost halved when openings were introduced on the 4,200 mm long masonry walls. In addition, by comparing the lateral strengths of Walls 6 and 7, it is shown that the introduction of a door opening resulted in the reduction of strength from 94 to 83 kN in Wall 7 (about 12% reduction of strength). Note that test results of Walls 4, 5, and 8 are not included in Figs. 7 and 9 because the detailing of trimming reinforcement in these walls differed from that specified in NZS 4229.

Effect of Trimming Reinforcement

Experimental results illustrated that the use of extended D16 trimming reinforcement affected wall strength considerably. This increase of wall strength can also be identified in the force-displacement envelopes presented in Figs. 10 and 11. Fig. 10 shows the force-displacement envelopes for Walls 2, 4, and 5. These three partially grout-filled masonry walls were constructed to identical geometries and consisted of identical longitudinal and bond beam reinforcement, with the only difference being the length of trimming reinforcement used in each wall. The trimming reinforcement in Wall 2 (see Fig. 1) was detailed according to the specifications of NZS 4229, but Walls 4 and 5 were detailed with extended trimming reinforcement. As shown in Fig. 1, the

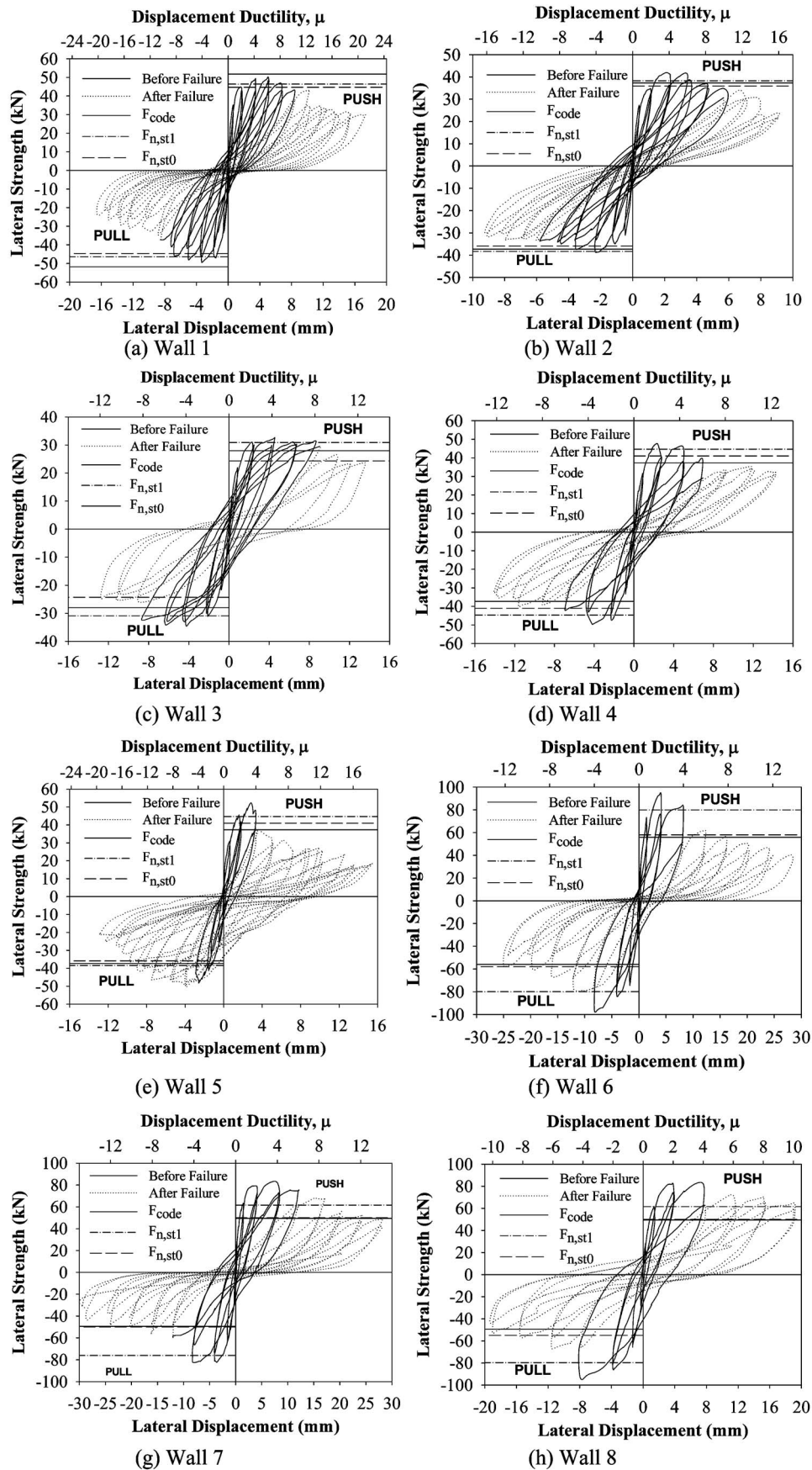


Fig. 5. Force displacement histories

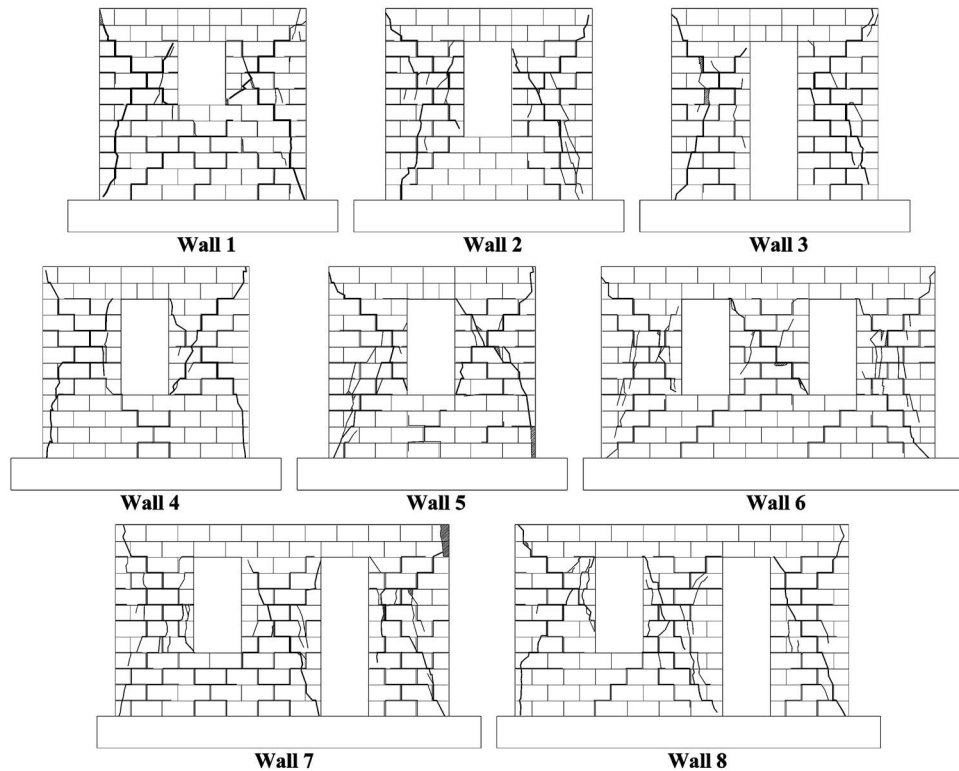


Fig. 6. Masonry wall cracking patterns

trimming reinforcement in Wall 5 was only extended to the outermost vertical reinforcement on one side of the wall, therefore resulting in higher strength being predicted in the push direction than in the pull direction.

The force-displacement envelopes in Fig. 10 clearly illustrate the increase of lateral strength from the maximum of 41.2 kN for Wall 2 to 47.7 and 52.4 kN when the trimming reinforcement was extended beneath the window opening in Walls 4 and 5, therefore resulting in strength increases of about 18% and 27%, respectively. Similar to Fig. 10, the force-displacement envelopes in Fig. 11 illustrate an increase in wall pull strength from 82.5 kN for Wall 7 to 93.2 kN when the trimming reinforcement of Wall 8 was extended to the outermost vertical reinforcement in the left pier (see Fig. 1), resulting in a pull direction strength increase of about 12%.

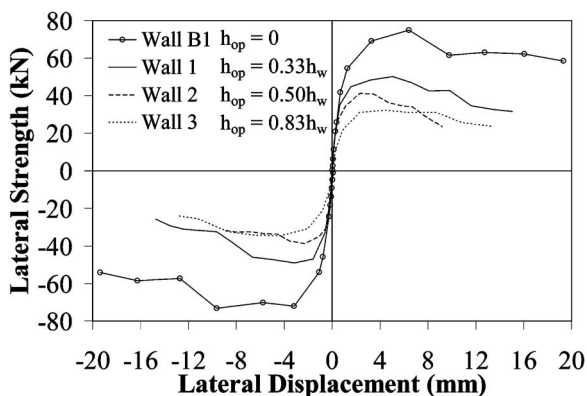


Fig. 7. Effect of opening on 2,600 mm long walls

Wall Strength Prediction

The test results presented in Table 1 clearly demonstrate that the size of openings and the arrangement of trimming reinforcement significantly affect the lateral strength of perforated masonry walls. For the small window opening in Wall 1, the measured strength was slightly less than that prescribed by NZS 4229, resulting in $F_{max}/F_{code}=0.95$. However, the results in Fig. 5 indicate that the conservatism of NZS 4229 increases with the height of opening, and for a full height opening (e.g., a door in Wall 3), the NZS 4229 prediction had significant conservatism.

Shown also in Fig. 5 is that a 50% increase in the number of piers for the 4,200 mm long walls resulted in approximately 100% increase in lateral strength when compared to the strengths recorded for the 2,600 mm long walls (compare Wall 6 to Wall 4). This is explained by considering the wall crack patterns shown in

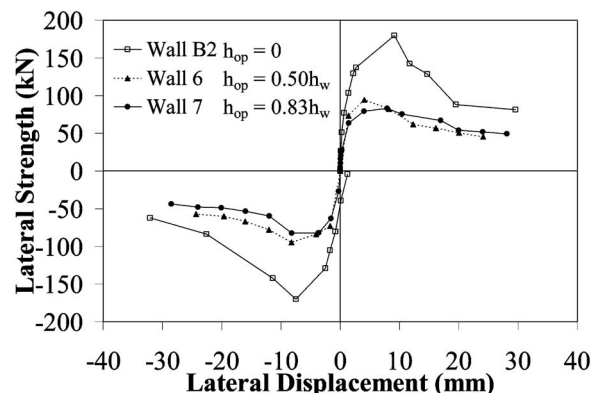


Fig. 8. Effect of openings on wall strength (shown for pull direction)

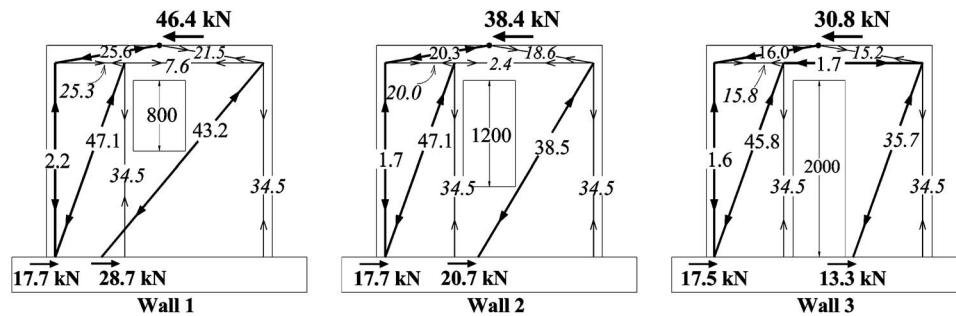


Fig. 9. Effect of openings on 4,200 mm long walls

Fig. 6, where it can be seen that diagonal cracks passed through the exterior lintel-pier joints of all walls, effectively resulting in a pinned connection at those locations, whereas all interior lintel-pier joints remained uncracked during testing and hence were capable of moment resistance. It is therefore established that double bending of the central pier significantly increased the lateral strength of perforated walls having interior piers. Consequently, failure of NZS 4229 to account for the extra strength generated by double bending of the central pier resulted in significant underprediction of strengths recorded in Walls 6–8. As shown in Table 1, ratios of $0.95 \leq F_{\max}/F_{\text{code}} \leq 1.40$ and $1.68 \leq F_{\max}/F_{\text{code}} \leq 1.89$ were observed for the 2,600 mm and 4,200 mm long perforated walls included in this study. This observation subsequently led to the conclusion that NZS 4229 is only nonconservative for walls containing a single opening with a height of less than 1,200 mm, but that the standard has considerable conservatism for walls that have more than one opening due to the inner piers undergoing double bending.

Comparisons of $F_{\max}/F_{n,\text{st}0}$ and $F_{\max}/F_{n,\text{st}1}$ are presented in Table 1. It is shown that the simplified strut-and-tie method adequately predicted the lateral strength of the 2,600 mm long perforated masonry walls, with $F_{\max}/F_{n,\text{st}0}$ varying from 1.12 to 1.28 (excluding the experimental result obtained in the pull direction for Wall 5). However, the effectiveness of this method was significantly reduced when predicting the strengths of the 4,200 mm long masonry walls included in this study. This was shown by the consistent underprediction of strengths for Walls 6–8 by about 60% when the simplified strut-and-tie method was used. Similar to NZS 4229, this underprediction of wall strength was due to the fact that double bending of the central pier was not accounted for in the simplified strut-and-tie models.

To address this identified fault in NZS 4229 it is proposed that a strength reduction factor of 0.8 be applied to panels having a height of 0.8 m and a similar factor of 0.9 be applied to panels having a height of 1.2 m. These recommended changes have been incorporated into Table 3, and are also identified in Table 1 by the ratio $F_{\max}/F_{\text{code}}^*$. From Table 1, it may be established that these recommended alterations to the standard then result in comparable levels of conservatism for the range of window openings considered in this study.

For the improved strut-and-tie method, it is illustrated in Fig. 3 that significantly improved strength predictions were attained when double bending of the central pier and when wall self-weight were considered in models presented in Fig. 4(b), resulted in average $F_{\max}/F_{n,\text{st}1}$ values of about 1.10 for the 2,600 mm long walls (excluding Wall 5 pull direction) and 1.22 for the 4,200 mm long masonry walls. The diagonal cracking patterns illustrated in Fig. 6 were observed to align well with the load paths by which lateral force was assumed to be transferred to the foundation in the strut mechanism. This observation supports use of the strut-and-tie method as the tool to evaluate the strength of nominally reinforced masonry walls with openings.

Conclusions

It was observed that the perforated partially grouted concrete masonry walls tested at the University of Auckland exhibited gradual strength and stiffness degradation, and in no case did any wall suffer from sudden failure. This desirable behavior of the nominally reinforced partially grouted masonry walls with openings was attributed to the solid filled bond beam at the top of the walls,

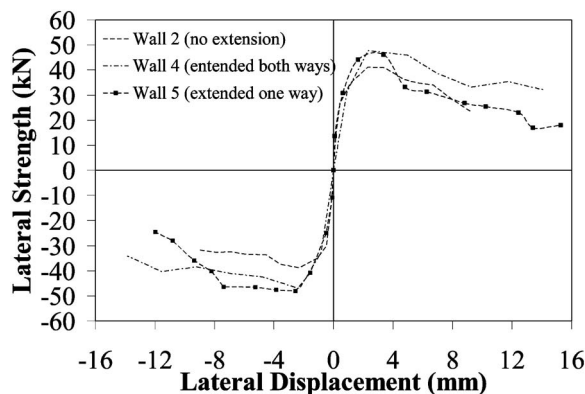


Fig. 10. Effect of trimming reinforcement on 2,600 mm long perforated masonry walls

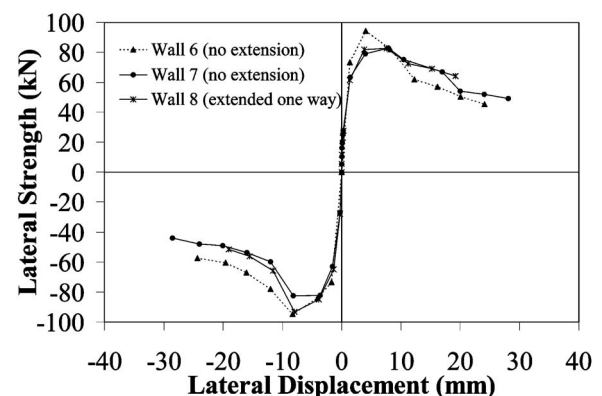


Fig. 11. Effect of trimming reinforcement on 4,200 mm long perforated masonry walls

Table 3. Recommended Bracing Capacities (kN) for 140 mm Partially Grouted Concrete Masonry

Panel height (m)	Panel length (m)								
	0.8	1.2	1.6	2.0	2.8	3.6	4.4	5.2	6.0
0.8	15.4	26.0	40.2	57.0	100.2	124.4	178.2	241.6	314.8
1.2	12.4	21.1	32.9	46.6	82.2	102.0	146.3	198.7	258.8
2.0	9.0	15.3	24.0	34.0	60.3	75.0	107.8	146.5	191.3
3.0	6.3	10.8	17.0	24.5	43.5	54.3	78.0	106.3	139.0

which caused frame-type action at latter stages of testing and permitted double bending to develop in the central piers of walls with two openings. This led to considerable inelastic displacement, where μ_{av} was consistently measured to be above 2.0. In addition, it was observed that maximum strength was typically developed during the first excursion to $\mu=4.0$. Following this, cracking became significant in the masonry walls and strength degradation began.

The test results clearly demonstrated that the size of openings significantly affected the lateral strength of the tested walls. It was shown that the reduction of wall strength corresponded to the increased height of an opening. This reduction of strength was because of the steepened diagonal strut when the height of openings increased. This in turn led to a reduction of the horizontal shear component that could be resisted by the masonry piers, which resulted in the overall reduction of lateral strength in the perforated masonry walls. In addition, it was demonstrated that extension of the trimming reinforcement below the window had the effect of increasing wall strength. It was also observed that the wall cracking pattern was altered when the trimming reinforcement was extended below the window opening.

It was established that NZS 4229 fails to correctly identify the geometry of bracing panels of perforated masonry walls, resulting in the overprediction of strength of walls containing a small opening. This was rectified by proposing a reduction to the assigned capacities of bracing panels having a height not greater than 1.2 m. It was shown in the experimental study that the conservatism of NZS 4229 increased when the height of opening is increased and when a wall contains more than one opening.

The diagonal cracking patterns on the perforated masonry walls were observed to align well with the load paths by which shear force was assumed to be transferred to the foundation in the strut mechanism. This observation supported use of the strut-and-tie method of analysis as the tool to evaluate the strength of nominally reinforced masonry walls with openings. Strength prediction using the improved strut-and-tie method was found to closely match the experimental results of walls having more than one opening. Strength prediction by the simplified strut-and-tie method was found to closely match the test results of masonry walls with a single opening, but significant underestimation of strength by this method was found for walls with two openings

Acknowledgments

This research was funded by the Earthquake Commission Research Foundation (EQC). Materials and construction labor associated with the testing of masonry walls was provided by Firth Industries Ltd., W. Stevenson and Sons Ltd., and Ready Mix Concrete Ltd. Their contributions are gratefully acknowledged. The writers also wish to acknowledge contributions by Hank Mooy and Tony Daligan, who were responsible for the practical aspects in relation to testing of the wall specimens in the Civil Test Hall

of the University of Auckland. The opinions and conclusions presented herein are those of the writers, and do not necessarily reflect those of the University of Auckland or any of the sponsoring parties to this project.

Notation

The following symbols are used in this paper:

- F_{code} = NZS 4229 code specified wall nominal strength;
- F_{code}^* = updated NZS 4229 code specified wall nominal strength including correction factor for openings of 0.8 m and 1.2 m;
- F_{max} = maximum experimentally measured strength;
- F_n = nominal flexural strength;
- $F_{n,st0}$ = nominal wall strength according to simplified strut-and-tie model;
- $F_{n,st1}$ = nominal wall strength according to improved strut-and-tie model;
- f'_m = masonry compressive strength;
- f_y = yield strength of reinforcement;
- h_{op} = height of opening;
- h_w = height of wall;
- L_w = length of wall;
- Δ_y = nominal yield strength;
- μ = displacement ductility level;
- μ_{av} = available displacement ductility factor;
- μ_{max} = displacement ductility level corresponding to maximum strength; and
- ϕ = strength reduction factor.

References

- Brammer, D. R. (1995). "The lateral force-deflection behaviour of nominally reinforced masonry walls." MS thesis, Dept. of Civil and Resource Engineering, Univ. of Auckland, New Zealand.
- Davidson, B. J. (1996). "In-plane cyclic loading of nominally reinforced masonry walls with openings." *Proc., New Zealand Concrete Society Conf.*, Wairakei, New Zealand, 120–129.
- Dowrick, D. J. (1998). "Damage and intensities in the magnitude 7.8 1931 Hawke's Bay, New Zealand earthquake." *Bull. New Zealand National Society for Earthquake Engineering*, 30(2), 139–162.
- Ingham, J. M., Davidson, B. J., Brammer, D. R., and Voon, K. C. (2001). "Testing and codification of partially grout-filled nominally-reinforced concrete masonry subjected to in-plane cyclic loads." *Masonry Soc. J.*, 19(1), 83–96.
- NZS. (1999). "Concrete masonry buildings not requiring specific engineering design," *NZS 4229*, Standards Association of New Zealand, Wellington, New Zealand.
- NZS. (2004). "Design of reinforced concrete masonry structures," *NZS 4230*, Standards Association of New Zealand, Wellington, New Zealand.
- Scott, E. F. (1999). "A report on the relief organisation in Hastings arising

- out of the (magnitude 7.8) earthquake in Hawke's Bay [New Zealand] on February 3, 1931." *Bull. New Zealand National Society for Earthquake Engineering*, 32(4), 246–256.
- Voon, K. C., and Ingham, J. M. (2006). "Bracing capacity of partially grouted concrete masonry walls with openings," *School of Engineering Rep. No. 629*, University of Auckland, New Zealand.
- Voon, K. C., and Ingham, J. M. (2007). "Design expression for the in-plane shear strength of reinforced concrete masonry." *J. Struct. Eng.*, 133(5), 706–713.
- Wu, H., and Li, B. (2003). "Investigating the load paths of RC shear wall with openings under reversed cyclic loadings." *Proc., Pacific Conf. on Earthquake Engineering* (CD-ROM), Christchurch, New Zealand, Paper No. 123, 1–9.
- Yanez, F. V., Park, R., and Paulay, T. (1991). "Seismic behaviour of reinforced concrete structural walls with irregular openings." *Proc., Pacific Conf. on Earthquake Engineering*, New Zealand, 3303–3308.